PHYSICAL REVIEW B VOLUME 52, NUMBER 19 15 NOVEMBER 1995-I

Influence of a polarizable medium on the nonlocal optical response of a metal surface

A. Liebsch
Institut für Festkörperforschung, Forschungszentrum Jülich, 52425 Jülich, Germany

W.L. Schaich
Physics Department, Indiana University, Bloomington, Indiana 47405
(Received 19 June 1995)

The nonlocal optical response of a metallic surface is evaluated for a two-component *s-d* electron system with the aim of achieving a qualitative representation of the electronic surface excitations of Ag. The *s* electrons are treated as a semi-infinite homogeneous electron gas while the effect of the fully occupied *d* bands is simulated by a polarizable medium. According to the more localized nature of the *d* states, this polarizable medium is assumed to extend only up to a certain distance from the surface. Since the *s* electrons spill out farther into the vacuum, the *s-d* screening interaction in the surface region is less pronounced than in the bulk. Using time-dependent local-density calculations, it is shown how the profile of induced surface charge density and the dispersion of the surface plasmon change with the amount of *s-d* screening allowed. A key to these calculations is the derivation of a sum rule expression for the centroid of the induced surface charge in the *s-d* system.

I. INTRODUCTION

There exists now a wealth of knowledge about the electronic excitations at simple metal surfaces.[1] For example, the wave vector dispersion of the monopole and multipole surface plasmons has been measured for a variety of systems and semi-quantitative agreement with calculations using the time-dependent density functional approach has been achieved.[2] The nonlocal linear and nonlinear optical response of simple metal surfaces is also reasonably well understood.[3,4] The basis of the theoretical progress is the weakness of the ionic pseudopotentials in these systems. The dominant surface excitations can, therefore, be represented by those of the homogeneous semi-infinite electron gas. Because of the one-dimensional nature of the effective one-electron potential, the electronic ground state density profile and the various induced surface charge densities can now be computed quite easily. Moreover, the time-dependent local-density approximation (TDLDA) (Ref. 5) seems to provide a sufficiently accurate picture of the electronic correlations in the presence of finite-frequency external electric fields. Analogous calculations that include crystallinity effects are considerably more demanding and have been carried out only for special cases.[6] On the other hand, many surface spectroscopic measurements in the past were performed on noble and transition metals where interband transitions caused by the lattice potential must be taken into consideration. Thus, there is an obvious need to go beyond the theoretical description of nearly free-electron systems.

A striking manifestation of the important influence of shallow bound states on the surface excitation spectra is the dispersion of the Ag surface plasmons with parallel momentum q.[7] As result of the mutual *s-d* polarization, the frequency of the surface plasmon at $q = 0$ is reduced from the nominal free-electron value at 6.5 eV to about 3.7 eV. Moreover, instead of the familiar negative dispersion at small q of the surface plasmon on simple metal surfaces,[2,8] the Ag surface plasmon shows a positive dispersion at all wave vectors.[7] Large redshifts are also observed for the Ag volume plasmon[9] and the Mie resonance of Ag particles.[10] This lowering of the Ag collective excitations can be nicely understood in terms of the picture suggested by Ehrenreich and Philipp,[9] who wrote the volume dielectric function $\epsilon(\omega)$ as a superposition of a Drude term $\epsilon_s(\omega)$ from the *s-p* electron states and a bound term $\epsilon_d(\omega)$, due to the filled *d* bands. Thus, $\epsilon(\omega) = \epsilon_s(\omega) + \epsilon_d(\omega) - 1$. The volume, surface and Mie plasmons are then given by the conditions $\epsilon(\omega) = 0$, $\epsilon(\omega) = -1$, and $\epsilon(\omega) = -2$, respectively. Since $\epsilon_d(\omega) \approx 5 \cdots 6$ in the vicinity of the collective modes, their frequencies are $\omega_p^* = \omega_p/\sqrt{\epsilon_d} \approx 3.76$ eV, $\omega_s^* = \omega_p/\sqrt{\epsilon_d + 1} \approx 3.63$ eV, $\omega_M^* = \omega_p/\sqrt{\epsilon_d + 2} \approx 3.50$ eV, where $\omega_p = 9.2$ eV is the bulk plasma frequency of the *s* electron density alone.

Recently, Liebsch[11] has shown that the *s-d* polarization interaction can also explain the positive dispersion of the Ag surface plasmon and the blueshift of the Ag Mie resonance as a function of decreasing particle size.[12] Since the *d* electrons are more tightly bound, they do not spill out as far into the vacuum as the *s-p* states. Thus, in the surface region, the *s-d* polarization is reduced compared to its strength in the interior. At finite parallel wave vectors q, the fluctuating charge density associated with the surface plasmon, therefore, oscillates at a higher frequency than in the $q = 0$ limit, where the full *s-d* interaction applies. With increasing q, this upward shift becomes progressively more pronounced since the induced electric field decays more rapidly into the bulk. Time-dependent LDA calculations for this combined *s-d*

0163-1829/95/52(19)/14219(16)/$06.00

electron response show that the q-dependent screening reduction is indeed large enough to qualitatively reproduce the experimentally observed Ag surface plasmon dispersion. In these calculations, the s electrons are treated as a semi-infinite jellium system and the occupied d bands are represented via a polarizable half space, which extends up to a certain distance z_d near the surface. The local dielectric function $\epsilon_d(\omega)$ of this medium is assumed to be the same as in the bulk. The attractive feature of this model is that it retains the computational simplicity of one-dimensional jellium systems, while capturing an essential aspect of the dynamical response of metals with shallow occupied states.

The surface response calculations performed in Ref. 11 are numerically stable down to q values of about 0.05 Å^{-1} and the Ag surface plasmon dispersion extrapolates well to the expected value ω_s^* in the long wavelength limit. Nevertheless, the precise determination of the initial slope of the dispersion is difficult, since it is *a priori* not clear over which q range a linear expansion is valid. In fact, the TDLDA results for $z_d = 0$ (when the polarizable medium extends up to the edge of the positive background) indicate a weak minimum in $\omega_s^*(q)$ at $q < 0.05$ Å^{-1}. This result suggests that the linear region is rather small. It also implies that the main part of the positive dispersion observed experimentally up to 0.3 Å^{-1} need not be related to the linear coefficient at small q. For $z_d < 0$, the initial slope of $\omega_s^*(q)$ becomes positive and the overall dispersion agrees qualitatively with the experimental results.[7]

The aim of the present work is to investigate further the nonlocal optical response within the two-component s-d electron model outlined above. In particular, we evaluate the frequency dependence of the centroid $d_\perp(\omega)$ of the induced surface charge in the long wavelength limit. This function is relevant for the so-called nonlocal corrections to the standard Fresnel reflectivity formulas and for the small-q behavior of the surface plasmon.[13,14] An important conclusion from our results is that the polarizable medium representing the Ag d bands leads to a frequency dependent inward shift of the centroid $d_\perp(\omega)$. This shift becomes particularly pronounced just below the volume plasma frequency ω_p^*. Near ω_s^*, however, $\mathrm{Re}\, d_\perp(\omega)$ is still positive if $z_d = 0$, i.e., the induced charge centroid remains located outside the jellium edge. If the boundary z_d is moved inside, $\mathrm{Re}\, d_\perp(\omega_s^*)$ becomes negative. These results are consistent with the finite-q surface plasmon dispersion investigated in Ref. 11. These results also underscore the cautionary point raised above, namely, that the main region of the measured dispersion cannot be used to determine the linear coefficient in the $q \to 0$ limit.

The influence of bound states on the dynamical response at metal surfaces has been investigated previously by several authors. In their work on the surface corrections to the van der Waals attraction, Zaremba and Kohn[15] represented the centroid $d_\perp$ of the total induced electronic density by a weighted average of the s and d contributions, d_s and d_d, which were taken from independent calculations for a jellium model and a dielectric solid, respectively:

$$d_\perp(iu) = \frac{\epsilon_s(iu) - 1}{\epsilon(iu) - 1}\, d_s(iu) + \frac{\epsilon_d(iu) - 1}{\epsilon(iu) - 1}\, d_d(iu)\ . \quad (1)$$

At the imaginary frequencies needed for the van der Waals case, this approach is reasonable since the external fields at the positions of the ion cores are rapidly screened by the jellium component. As shown in Ref. 15, $d_d(iu) \approx 0$ for the (100) face of a simple cubic lattice of point dipoles. If the s electrons are treated as a Drude metal, one finds

$$d_\perp(iu) = \frac{\epsilon_s(iu) - 1}{\epsilon(iu) - 1}\, d_s(iu) = \frac{d_s(iu)}{1 + [\epsilon_d(iu) - 1]u^2/\omega_p^2}\ . \quad (2)$$

Thus, the charge centroid is shifted inwards but it remains located outside the jellium surface at all imaginary frequencies.

In the optical case, this picture breaks down, since the fields penetrate the metal and the s and d electron responses cannot be treated as independent of one another. Apell and Holmberg[16] argued that at optical frequencies, one should modify the weight factor in (2), so that

$$d_\perp(\omega) = \frac{\epsilon_s(\omega) - 1}{\epsilon(\omega) - 1}\, \frac{\epsilon(\omega)}{\epsilon_s(\omega)}\, d_s(\omega)\ . \quad (3)$$

This centroid approaches the jellium surface at the Ag bulk plasma frequency. However, since the bulk plasmon also defines the transparency threshold of the metal, $d_\perp(\omega)$ should not remain localized at the surface, but instead (in the absence of damping) go to $-\infty$.

All of the models discussed so far are purely one dimensional. Thus, the crystal face dependence of the Ag surface plasmon dispersion and its anisotropy on the (110) face[7] cannot easily be addressed within these models. In an effort to understand such phenomena, Tarriba and Mochan[17] followed a different approach. They describe the s-d electron system by a semi-infinite lattice of point dipoles immersed in a local Drude system with cavities at the lattice points. The s electron density is abruptly terminated at the surface. The d parameters obtained within this model differ for the three low-index faces. This model was also used to analyze the reflection anisotropy observed on Ag(110).[18]

Finally, Feibelman[19] discussed the influence of s-d matrix elements on $d_\perp(\omega)$, by considering a surface perturbation to the Lang-Kohn potential.[20] Since an extra potential well increases the local electron density near the surface, and since high-density metals have less polarizable density profiles, the magnitude of $d_\perp(\omega)$ should diminish. Thus, the initial slope of the surface plasmon should be less negative than in the unperturbed jellium model. In the $q = 0$ limit, this model yields the unscreened plasma frequency $\omega_s = 6.5$ eV, since the long-range s-d polarization interaction is not taken into account. The matrix elements should become stronger with decreasing separation between the fluctuating s charge and the d states. Thus, this model predicts successively less negative slopes for the (111), (100), and (110) faces of Ag. Such a trend is indeed observed between the (111)

and (100) faces, but the two slopes for Ag(110) lie in between those for Ag(111) and (100).[7,21]

The structure of this paper is as follows. In Sec. II, we specify the model and describe the real-space solution of the response equation for the induced surface density. Because of the long-range nature of the Coulomb potential in the $q = 0$ limit and the slow decay of the Friedel oscillations of the induced density, the charge centroid $d_\perp(\omega)$ can be reliably evaluated only if one makes use of the dynamical force sum rule.[22,23] The extension of this sum rule to the two-component s-d electron system is presented in Sec. III. The results are discussed in Sec. IV and Sec. V contains a summary.

II. FORMALISM

In principle, the occupied Ag $4d$ bands can affect the dynamical surface response in two ways: (i) the s-d hybridization modifies the single-particle wave functions and energies so that the nonlocal density-density response function exhibits band structure effects; (ii) the effective time-varying fields are modified, due to the mutual polarization of the s and d electron densities. A full numerical treatment of both of these effects is not yet feasable. Since close to the Fermi level the Ag energy bands are nearly free-electron like and since the Ag surface plasmon lies below the region of interband transitions, we neglect the band structure effects and focus on the s-d polarization. Excitations involving the filled d states enter, therefore, only as virtual transitions, which we describe in terms of a polarizable medium that extends up to some distance z_d from the surface. Thus, we write $\epsilon_d(z,\omega) = \epsilon_d(\omega)$ for $z < z_d$ and $\epsilon_d(z,\omega) = 1$ for $z > z_d$ (see Fig. 1). We assume that the s-electron

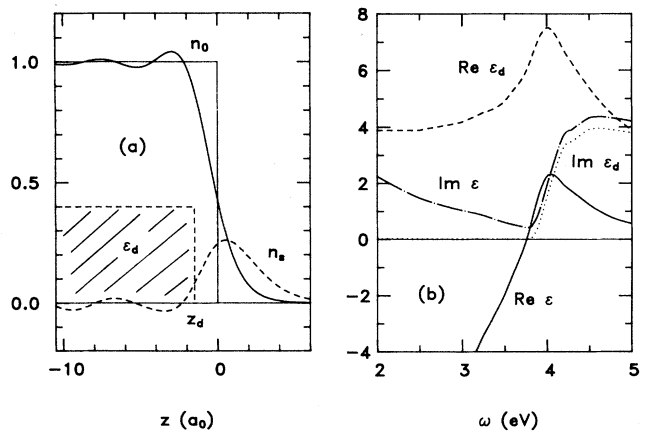

FIG. 1. (a) Schematic model for the dynamical response of a two-component s-d electron system. Solid curve: ground state density profile of the s electrons; dashed curve: induced density. The positive background is located in the space $z \leq 0$; the polarizable medium, due to the d states, extends up to $z \leq z_d$. (b) Frequency dependence of the real and imaginary parts of the "bound" dielectric function $\epsilon_d(\omega)$ (dashed and dotted curves, respectively). The measured dielectric function of bulk Ag (Ref. 26) is also shown: solid and dot-dashed curves for its real and imaginary parts.

response can be characterized by the nonlocal surface response function of a semi-infinite jellium system. The neutralizing positive background is located in the half space $z \leq 0$.

Let us consider the density response to a uniform electric field oriented perpendicular to the surface and oscillating in time as $\sim \exp(-i\omega t)$. The spatial part of the associated electric potential is assumed to be given by $\phi_{\rm ext}(z) = -2\pi z$. Within the TDLDA, the induced density of the s electrons can be obtained from the response equation,

$$\delta n_s(z,\omega) = \int dz'\, \chi_1(z,z',\omega) \left[\phi_{\rm ext}(z') + \delta\phi(z',\omega) + \delta V_{\rm xc}(z',\omega)\right] , \tag{4}$$

where $\chi_1(z,z',\omega)$ is the $q = 0$ limit of the jellium independent-particle susceptibility and $\delta\phi$ is the induced Coulomb potential. In the adiabatic version of the TDLDA,[5] the induced exchange-correlation contribution is obtained from the ground state exchange-correlation functional via

$$\delta V_{\rm xc}(z,\omega) = [\partial V_{\rm xc}(n)/\partial n]|_{n_0(z)}\ \delta n_s(z,\omega) . \tag{5}$$

Henceforth, for simplicity, we will usually not show the ω dependence of functions.

The total electrostatic potential $\phi = \phi_{\rm ext} + \delta\phi$ determines the total electric field $E = -\phi' = E_{\rm ext} + \delta E$, which in turn satisfies Gauss's law,

$$E' = -\phi'' = 4\pi\delta n = 4\pi(\delta n_s + \delta n_d) . \tag{6}$$

Further reduction now depends on how one deals with the induced density of the d electrons, $\delta n_d(z)$. We describe two derivations that use different mathematical treatments of δn_d, but eventually lead to the same effective response equation to be solved numerically.

First approach

To begin the first procedure, we write $\delta n_d = -P_d'$, where $P_d(z)$ is the polarization of the d electrons, and rearrange (6) to

$$(E + 4\pi P_d)' = 4\pi\delta n_s , \tag{7}$$

or, after introducing $\epsilon_d(z)$,

$$(\epsilon_d\phi')' = -4\pi\delta n_s . \tag{8}$$

To solve (8) for all z, we combine solutions of

$$\epsilon_d\phi'' = -4\pi\delta n_s , \tag{9}$$

for $z \neq z_d$, with the boundary condition across z_d of

$$\epsilon_d\phi'(z_d^-) = \phi'(z_d^+) , \tag{10}$$

where $z_d^\pm \equiv z_d \pm 0^+$. We write the induced Coulomb potential as $\delta\phi = \phi_1 + \phi_2$, with

$$\phi_1(z) = -2\pi \int dz' \, |z - z'| \, \delta n_s(z')/\epsilon_d(z') \, , \tag{11}$$

$$\phi_2(z) = -2\pi \, |z - z_d| \, a \, . \tag{12}$$

The expression for ϕ_1 follows from the Poisson equation (9), while the extra term ϕ_2 arises from the sheet of screening charge in the $z = z_d$ plane. The coefficient a may be determined as follows. Let us define

$$\phi_1'(z_d) = -2\pi \int dz' \, \delta n_s(z') \, \mathrm{sgn}(z_d - z') \, /\epsilon_d(z') \equiv -2\pi \, b \, . \tag{13}$$

From (12), we have $\phi_2'(z_d^{\pm}) = \mp 2\pi a$, which gives $\phi'(z_d^{\pm}) = -2\pi \, (1 + b \pm a)$. The condition (10) then implies

$$a = (1 + b) \, \frac{\epsilon_d - 1}{\epsilon_d + 1} \equiv (1 + b) \, \bar{\sigma}_d \, . \tag{14}$$

Far from the surface, the total Coulomb potential is given by

$$\phi(z) \to -2\pi \left(z \pm \sigma \, [z - d_\perp] \right) \, , \qquad z \to \pm\infty \, , \tag{15}$$

where

$$\sigma = a + \int dz \, \delta n_s(z)/\epsilon_d(z) = \bar{\sigma}_d + \frac{2\sigma_s}{\epsilon_d + 1} \tag{16}$$

and

$$d_\perp = \frac{1}{\sigma} \left(a z_d + \int dz \, z \, \delta n_s(z)/\epsilon_d(z) \right) = z_d + \frac{1}{\sigma} \int dz \, (z - z_d) \, \delta n_s(z)/\epsilon_d(z) \, . \tag{17}$$

Here, a is defined in (14) and σ_s is the integrated weight of the induced density $\sigma_s = \int dz \, \delta n_s(z)$. Using the boundary condition $\epsilon \, \phi'(-\infty) = \phi'(\infty)$, we also can express σ as

$$\sigma = \frac{\epsilon - 1}{\epsilon + 1} \, , \tag{18}$$

which yields

$$\sigma_s = \frac{\epsilon_s - 1}{\epsilon + 1} \, . \tag{19}$$

In analogy, we introduce the quantity

$$\sigma_d = \frac{\epsilon_d - 1}{\epsilon + 1} \, , \tag{20}$$

so that $\sigma = \sigma_s + \sigma_d$.

In order to explicitly account for the asymptotic behavior of the Coulomb potential, we separate the long-range bulk part and write

$$\phi(z) = \phi_b(z) + \phi_r(z) \, , \tag{21}$$

where the bulk part is

$$\phi_b(z) = -2\pi \left(z - \sigma \, [z - d_\perp] \right) \, , \tag{22}$$

nd the remainder is

$$\phi_r(z) = -4\pi \int_{-\infty}^{z} dz'(z - z') \frac{\delta n_s(z')}{\epsilon_d(z')} - 4\pi \, (z - z_d) \, a \, \theta(z - z_d) \, . \tag{23}$$

Here, $\theta(z \geq 0) = 1$ and $\theta(z < 0) = 0$. With the above definitions, we can rewrite (4) as

$$\delta n_s(z) = \delta \bar{n}_s^B(z) + \int dz' \, \chi_1(z, z') \left(\phi_r(z') + \delta V_{\mathrm{xc}}(z') \right) \, , \tag{24}$$

with

$$\delta \bar{n}_s^B(z) = \int dz' \, \chi_1(z, z') \, \phi_b(z') \, . \tag{25}$$

According to the definition (23), $\phi_r(z)$ vanishes for $z \ll 0$, i.e., this potential contribution is finite only in the surface region. The response equation (24) can, therefore, be solved in a computationally stable manner. The structure of this equation is the same as that for the simple metals discussed in Ref. 23. We may, therefore, use a similar procedure to solve for the induced density.

Second approach

Our second method for reducing (4–6) to a computationally tractable form is based on a formalism that was developed for tight-binding model calculations[24] and has been recently adapted to systems with arbitrary (but one-dimensional) crystallinity.[25] It initially treats the d-electron response as an active degree of freedom rather than as a passive screening function, but in the final integral equation that must be numerically solved [see (43) below] only the s-electron density response appears.

One begins with (4) for the s electrons and

$$n_d p(z, \omega) = P_d(z, \omega) = n_d \alpha(\omega) \, \theta(z_d - z) \, [E_{\mathrm{ext}} + \delta E(z, \omega)] \tag{26}$$

for the d electrons. Here, $\alpha(\omega)$ is the polarizability and $p(z, \omega)$ is the induced dipole moment of a d electron at z. Our continuum approximation for the d electrons allows no z dependence for the polarizability, aside from the cutoff by the θ function at z_d, and no local field factors. We can, hence, replace the product of α times the equilibrium density for d electrons, n_d, with

$$n_d \alpha(\omega) = [\epsilon_d(\omega) - 1]/4\pi. \tag{27}$$

Coupling between the s- and d-electron response occurs, because there are both s and d contributions to $\delta\phi$ and $\delta E = -\delta\phi'$. For the latter, one has $\delta E = \delta E_s + \delta E_d$, where (again suppressing ω dependence)

$$\delta E_s(z) = 2\pi \int dz' \ \mathrm{sgn}(z - z') \ \delta n_s(z') \ , \tag{28}$$

and

$$\delta E_d(z) = 2\pi \int dz' \ \mathrm{sgn}(z - z') \ \delta n_d(z') \ , \tag{29}$$

with

$$\delta n_d(z) = -n_d p'(z). \tag{30}$$

Integrating by parts in (29) yields

$$\delta E_d(z) = 2\pi n_d p_B - 4\pi n_d p(z), \tag{31}$$

where $p_B = p(z \to -\infty)$ is the bulk value of the dipole moment. In turn p_B can be determined from

$$n_d p_B = (\epsilon_d - 1) E_B / 4\pi \ , \tag{32}$$

where the bulk electric field is

$$E_B = E_{\mathrm{ext}}[1 - (\sigma_s + \sigma_d)] \ , \tag{33}$$

with the σ's given by (19,20). Now subtract (32) in $z < z_d$ from (26) to obtain

$$n_d \Delta p(z) = n_d \alpha \theta(z_d - z) \ \Delta E(z) \ , \tag{34}$$

where $\Delta p(z) = p(z) - p_B$ is nonzero only for $z < z_d$ and from (28–31)

$$\begin{aligned} \Delta E(z) &= E_{\mathrm{ext}} + \delta E(z) - E_B \\ &= 4\pi \int_{-\infty}^{z} dz' \ [\delta n_s(z') + \delta n_d(z')] \\ &= 4\pi \int_{-\infty}^{z} dz' \ \delta n_s(z') - 4\pi n_d \Delta p(z) \\ &\quad + 4\pi n_d p_B \theta(z - z_d) \ . \end{aligned} \tag{35}$$

One can use (35) in (34) to express $\Delta p(z)$ in terms of δn_s alone:

$$4\pi n_d \Delta p(z) = (1 - 1/\epsilon_d) \ \theta(z_d - z) \ 4\pi \int_{-\infty}^{z} dz' \ \delta n_s(z'). \tag{36}$$

A slightly different subtraction procedure is applied to (4). Begin by defining the response to the uniform bulk field of (33) as

$$\delta \bar{n}_s^{(B)}(z) = \int dz' \ \chi_1(z, z') \ \phi_B(z') \ , \tag{37}$$

where to within a constant $\phi_B(z) = -zE_B$ and (37) gives the same result as (25). Then the analog of (34) is

$$\delta n_s(z) = \delta \bar{n}_s^{(B)}(z) + \int dz' \ \chi_1(z, z') \ \Delta\phi(z') \ , \tag{38}$$

where

$$\Delta\phi(z) = \delta V_{\mathrm{xc}}(z) + \Delta\phi_s(z) + \Delta\phi_d(z) \ , \tag{39}$$

with

$$\Delta\phi_s(z) = -4\pi \int_{-\infty}^{z} dz'(z - z') \ \delta n_s(z') \ , \tag{40}$$

$$\begin{aligned} \Delta\phi_d(z) = 4\pi &\int_{-\infty}^{z} dz' \ n_d \Delta p(z') \\ &-4\pi(z - z_d) n_d p_B \ \theta(z - z_d). \end{aligned} \tag{41}$$

The response to the second term in (41) is easily computed and we formally add it to (37) by defining

$$\begin{aligned} \delta n_s^{(B)}(z) = &\int dz' \ \chi_1(z, z') \ [\phi_B(z') \\ &-4\pi n_d p_B (z - z_d) \ \theta(z - z_d)]. \end{aligned} \tag{42}$$

The other term in (41) can via (36) be expressed in terms of δn_s, leading to the integral equation to be numerically solved,

$$\delta n_s(z) = \delta n_s^{(B)}(z) + \int d\bar{z} \int dz' \ \chi_1(z, \bar{z}) \ v(\bar{z}, z') \ \delta n_s(z') \ , \tag{43}$$

with

$$\begin{aligned} v(\bar{z}, z') = &[\partial V_{\mathrm{xc}}(n)/\partial n]_{n_s(z')} \ \delta(\bar{z} - z') \\ &-4\pi \ \theta(\bar{z} - z') \ [\bar{z} - z' + f(\bar{z}, z')] \ , \end{aligned} \tag{44}$$

where for $z' < \bar{z}$,

$$f(\bar{z}, z') = (1/\epsilon_d - 1) \begin{cases} \bar{z} - z', & z' < \bar{z} < z_d \\ z_d - z', & z' < z_d < \bar{z} \\ 0, & z_d < z' < \bar{z}. \end{cases} \tag{45}$$

The important feature of (43) is that $\int dz' \ v(\bar{z}, z') \ \delta n_s(z')$ vanishes as $\bar{z}$ moves into the bulk. This suppresses the difficulties with the long-range Coulomb potential. Equation (43) appears similar to (24). One can show that they are in fact equivalent. First change ϕ_b of (22) to

$$\tilde{\phi}_b(z) = \phi_b(z) - 4\pi(z - z_d) \ n_d p_B \ \theta(z - z_d) \ . \tag{46}$$

Then $\delta \bar{n}_s^{(B)}$ of (25) becomes $\delta n_s^{(B)}$ and ϕ_r of (23) must be replaced by

$$\tilde{\phi}_r(z) = \phi_r(z) + 4\pi(z - z_d) \ n_d p_B \ \theta(z - z_d) \ . \tag{47}$$

Since $a = n_d p(z_d)$, one has

$$\begin{aligned} \tilde{\phi}_r(z) = -4\pi &\int_{-\infty}^{z} dz'(z - z') \ \frac{\delta n_s(z')}{\epsilon_d(z')} \\ &-4\pi(z - z_d) \ n_d \Delta p(z_d) \ \theta(z - z_d) \ . \end{aligned} \tag{48}$$

The corresponding expression from (43–45) is

$$\begin{aligned} -4\pi &\int_{-\infty}^{z} dz' \ [z - z' + f(z, z')] \ \delta n_s(z') \\ &= -4\pi \int_{-\infty}^{z} dz'(z - z') \ \frac{\delta n_s(z')}{\epsilon_d(z')} \\ &\quad -4\pi(1 - 1/\epsilon_d)(z - z_d) \ \theta(z \\ &\quad -z_d) \int_{-\infty}^{z_d} dz' \ \delta n_s(z') \ . \end{aligned} \tag{49}$$

Finally, (36) shows that (48) and (49) are the same.

d parameters

We conclude this section by deriving expressions for the d parameters. We begin with $d_{\|}$. Since our model allows no variations in the response as one moves parallel to the surface plane, we can use the local optics formula,[13,14]

$$(\epsilon - 1)d_{\|} = \int_{-\infty}^{\infty} dz\, [\epsilon(z) - \epsilon_F(z)], \tag{50}$$

where with the matching plane at $z = 0$, the Fresnel variation is

$$\epsilon_F(z) = \theta(z) + \epsilon\theta(-z)\ , \tag{51}$$

while the microscopic (but local) variation is

$$\epsilon(z) = 1 + (\epsilon_s - 1)\ \theta(-z) + (\epsilon_d - 1)\ \theta(z_d - z). \tag{52}$$

We find

$$d_{\|} = z_d \left(\frac{\epsilon_d - 1}{\epsilon - 1}\right)\ . \tag{53}$$

Near the surface plasmon in Ag, $\epsilon \sim -1$, while $\epsilon_d \sim +5$ and $\epsilon_s \sim -5$. These values imply that $d_{\|} \sim -2z_d$, so as z_d is moved down into the metal, $d_{\|}$ shifts out into vacuum.

For $d_{\perp}$, we start from the general expression,[13,14]

$$d_{\perp} = \int_{-\infty}^{\infty} dz\, [P(z) - P_F(z)]/P(B)\ , \tag{54}$$

and separate the polarizations into their s and d contributions. Then

$$d_{\perp} = \frac{P_s(B)}{P(B)}\ d_s + \frac{P_d(B)}{P(B)}\ d_d\ , \tag{55}$$

where for the s electrons,

$$d_s = \int dz\, [P_s(z) - P_s^{(F)}(z)]/P_s(B)\ , \tag{56}$$

with $P_s^{(F)}(z) = P_s(B)\ \theta(-z)$ and

$$P_s(B) = \sigma_s = \int_{-\infty}^{\infty} dz\ \delta n_s(z) = \frac{\epsilon_s - 1}{4\pi} E_B\ . \tag{57}$$

Equations of the same form apply to the d-electron terms. Since $\delta n_s(z) = -P_s'(z)$, we can reexpress (56) after an integration by parts as

$$d_s = \int_{-\infty}^{\infty} dz\ z\ \delta n_s(z) \Big/ \int_{-\infty}^{\infty} dz\ \delta n_s(z)\ . \tag{58}$$

Thus, d_s is set by the centroid of $\delta n_s(z)$. A similar result holds for d_d, but we use an alternate form in our calculations based on

$$\begin{aligned} d_d &= \int_{-\infty}^{\infty} dz\, [p(z)/p_B - \theta(-z)] \\ &= z_d + \int_{-\infty}^{z_d} dz\ \Delta p(z)/p_B\ . \end{aligned} \tag{59}$$

This can be reexpressed by using (36), which we rewrite here as

$$\Delta p(z)/p_B = \frac{\epsilon_s - 1}{\epsilon_d}\ \theta(z_d - z) \int_{-\infty}^{z} dz'\ \delta n_s(z')/\sigma_s\ . \tag{60}$$

Then

$$\begin{aligned} d_d &= z_d + \frac{\epsilon_s - 1}{\epsilon_d \sigma_s} \int_{-\infty}^{z_d} dz(z_d - z)\ \delta n_s(z) \\ &= z_d - \frac{\epsilon_s - 1}{\epsilon_d}(d_s - z_d) \\ &\quad + \frac{\epsilon_s - 1}{\epsilon_d \sigma_s} \int_{z_d}^{\infty} dz(z - z_d)\ \delta n_s(z)\ . \end{aligned} \tag{61}$$

Substituting (58) and (61) into (55), we find

$$\begin{aligned} d_{\perp} &= \frac{\epsilon_s - 1}{\epsilon - 1}\ d_s + \frac{\epsilon_d - 1}{\epsilon - 1}\ d_d \\ &= z_d + \frac{\sigma_s}{\sigma}(d_s - z_d) + \frac{\sigma_d}{\sigma}(d_d - z_d) \\ &= z_d + \frac{\sigma_s}{\sigma\epsilon_d}(d_s - z_d) \\ &\quad + \frac{\epsilon_d - 1}{\epsilon_d \sigma} \int_{z_d}^{\infty} dz(z - z_d)\ \delta n_s(z)\ . \end{aligned} \tag{62, 63}$$

We note that (62) has the same structure as the formula (1) used by Zaremba and Kohn.[15] The important difference here is that the two centroids d_s and d_d are evaluated consistently within a response treatment for the two-component s-d electron system. As the first line of (61) shows, in our model d_d is in fact fully determined by an integral of the induced density $\delta n_s(z)$ in the region of the polarizable medium.

The form of $d_{\perp}$ in (63) is convenient for numerical evaluation, since the only integral that appears to require evaluations in the troublesome region of the Friedel oscillations is (58) for d_s. However, even d_s can be calculated more simply. The key is to make use of the dynamical force sum rule.[22] For ordinary jellium surfaces and within the TDLDA, this leads to the identity[23]

$$\sigma d_{\perp} = \int_{-\infty}^{\infty} dz\ z\ \delta n(z) = \frac{\epsilon - 1}{\epsilon} \int_{0}^{\infty} dz\ z\ \delta n(z)\ . \tag{64}$$

Thus, the total induced dipole moment is fully determined by the part outside the jellium edge. It is, therefore, not necessary to calculate the internal moment where the induced density exhibits slowly decaying Friedel oscillations. The extension of this force sum rule to the present two-component surface response will be derived in the following section.

III. DYNAMICAL FORCE SUM RULE

This sum rule follows from the equation of motion for the s electrons.[22] It is convenient for its derivation to initially work in a slab geometry and then later go over to the limit of large slab thickness to find an appropriate expression for a semi-infinite system. Also, for clarity, we will explicitly show in this section factors of an electron's

charge, $e < 0$, and all n's will be number densities. Imagine that the metal slab is centered on $Z = 0$ and placed between distant, parallel plates that produce a uniform applied field E_A at frequency ω. The system has translational invariance in planes perpendicular to $\hat{Z}$ and one has per unit area along $\hat{Z}$,

$$\frac{\partial}{\partial t}\mathcal{P}_s = F_s - \frac{1}{\tau}\mathcal{P}_s \ , \tag{65}$$

where $\mathcal{P}_s$ is the momentum of the s electrons and F_s is the sum of the coherent forces acting on them. The term with $1/\tau$ arises from incoherent scattering. We ignore the position dependence of such scattering, but will allow $1/\tau$ to depend on frequency.

At first order within the original version of LDA response for the s-d model[11] Eq. (65) becomes

$$-m\tilde{\omega}^2 \int_{-\infty}^{\infty} dZ\ Z\delta n_s(Z) = e\int_{-\infty}^{\infty} dz\ \{\delta n_s(Z)E_+(Z) + n_0(Z)[E_A + \delta E_d(Z)]\} \ , \tag{66}$$

where $\tilde{\omega}^2 = \omega(\omega + i/\tau)$. We have calculated the momentum from the time derivative of the dipole moment and expressed the net force in terms of products of charge densities and fields. The new symbol is E_+ for the field due to the positive background, whose constant charge density is $-en_B$ between $\pm L_+$. Newton's third law justifies the absence of any direct forces between s electrons and further allows us to rewrite (66) as

$$-m\tilde{\omega}^2 \int_{-\infty}^{\infty} dZ\ Z\delta n_s(Z) = e\int_{-\infty}^{\infty} dZ\ \{n_+(Z)[E_A + \delta E_s(Z) + \delta E_d(Z)] + [n_0(Z) - n_+(Z)][E_A + \delta E_d(Z)]\} \ . \tag{67}$$

The integrands here are all even functions of Z, so that we can switch to (positive) half-space integrals and replace $Z = L + z$, where L defines the nominal edge of the s-electron gas via

$$\int_0^{\infty} dZ\ n_0(Z) = Ln_B. \tag{68}$$

The induced density profiles for $Z \approx L$; i.e., $z \approx 0$, should agree for a thick slab, within an overall scale factor, with those near the surface of a semi-infinite metal. Our aim is to rewrite the above to exploit this fact.

We can eliminate the fields in the first square bracket on the right side of (67) by integrating by parts and using Gauss's law. At the same time, we switch to z as the integration variable and argument of the functions. With $L_+ = L + \Delta$ and $\omega_p^2 = 4\pi n_B e^2/m$, we obtain

$$-m\tilde{\omega}^2\left[L\int_{-L}^{\infty} dz\ \delta n_s(z) + \int_{-L}^{\infty} dz\ z\delta n_s(z)\right] = -m\omega_p^2\int_{-L}^{\Delta} dz\ z\delta n(z) + en_B\Delta[E_A + \delta E(\Delta)] + en_B LE_B + e\int_{-L}^{\infty} dz\ [n_0(z) - n_+(z)][E_A + \delta E_d(z)] \ . \tag{69}$$

The terms with explicit factors of L cancel by the following argument. One has for the integrated charge on the right side of the slab,

$$\sigma_s(L) = e\int_{-L}^{\infty} dz\ \delta n_s(z) = P_s(-L), \tag{70}$$

and as $L \to \infty$,

$$P_s(-L) \to P_s(B) = \frac{\epsilon_s - 1}{4\pi}E_B. \tag{71}$$

If we use the Drude dielectric function,

$$\epsilon_s = 1 - \omega_p^2/\tilde{\omega}^2 \ , \tag{72}$$

for the s-electron bulk response, we find with σ_s the large L, limit of $\sigma_s(L)$,

$$en_B E_B = -m\tilde{\omega}^2\int_{-\infty}^{\infty} dz\ \delta n_s(z) = -m\tilde{\omega}^2\sigma_s/e, \tag{73}$$

which simplifies (69) and makes the limit $L, L_+ \to \infty$ well defined. Also note that in this limit,

$$\int_{-\infty}^{\infty} dz\ [n_0(z) - n_+(z)] = -n_B\Delta \ , \tag{74}$$

$$en_B\delta E(\Delta) = -m\omega_p^2\int_{\Delta}^{\infty} dz\ \delta n(z) \ . \tag{75}$$

Equation (69) now becomes

$$-\frac{\tilde{\omega}^2}{\omega_p^2}\int_{-\infty}^{\infty} dz\ z\delta n_s(z) = -\int_{-\infty}^{\Delta} dz\ z\delta n(z) - \Delta\int_{\Delta}^{\infty} dz\ \delta n(z) + \int_{-\infty}^{\infty} dz\ f(z)\delta E_d(z)/4\pi e \ , \tag{76}$$

where $f(z) = [n_0(z) - n_+(z)]/n_B$. If the system were overall neutral, Δ would vanish, and if there were no d electrons, δn and δn_s would be the same. Then one would quickly find (64) from (76).

Returning to the general case, we seek to replace δE_d and to express δn in terms of δn_s alone. This may be accomplished by integrating the d-electron Poisson equation,

$$\frac{\partial}{\partial z}\delta E_d = 4\pi e\delta n_d = -4\pi\frac{\partial}{\partial z}P_d. \tag{77}$$

Since δE_d vanishes away from the slab in a capacitor geometry, one has

$$\delta E_d = -4\pi P_d \ . \tag{78}$$

For P_d, we use (near the right edge of the slab)

$$P_d(z) = \theta(z_d - z)\left[\frac{\epsilon_d - 1}{4\pi} E_B + \left(1 - \frac{1}{\epsilon_d}\right)\int_{-\infty}^{z} dz'\, e\delta n_s(z')\right] \tag{79}$$

and find δn_d by differentiation

$$\delta n_d(z) = \frac{1}{e} P_d(z_d)\delta(z - z_d) + \theta(z_d - z)(1/\epsilon_d - 1)\delta n_s(z) \ . \tag{80}$$

Before substituting these results back into (76), use (73) to remove $E_B/4\pi = -\tilde{\omega}^2\sigma_s/\omega_p^2$ from (79),

$$\frac{1}{e}P_d(z) = \theta(z_d - z)(\epsilon_d - 1)\left[-\frac{\tilde{\omega}^2}{\omega_p^2}\frac{\sigma_s}{e} + \frac{1}{\epsilon_d}\int_{-\infty}^{\infty} dz'\, \delta n_s(z')\right] . \tag{81}$$

Then, we obtain

$$-\frac{\tilde{\omega}^2}{\omega_p^2}\int_{-\infty}^{\Delta} dz\, z\delta n_s(z) = -\int_{-\infty}^{\infty} dz\, z\frac{\delta n_s(z)}{\epsilon_d(z)} - \Delta\int_{\Delta}^{\infty} dz\, \frac{\delta n_s(z)}{\epsilon_d(z)} + (1-\epsilon_d)\left\{\left[-\frac{\tilde{\omega}^2}{\omega_p^2}\frac{\sigma_s}{e} + \frac{1}{\epsilon_d}\int_{-\infty}^{z_d} dz'\, \delta n_s(z')\right][z_d\theta(\Delta - z_d) + \Delta\theta(z_d - \Delta)] + \int_{-\infty}^{z_d} dz\, f(z)\left[-\frac{\tilde{\omega}^2}{\omega_p^2}\frac{\sigma_s}{e} + \frac{1}{\epsilon_d}\int_{-\infty}^{z} dz'\, \delta n_s(z')\right]\right\} . \tag{82}$$

The θ functions arise from considering whether the singular contribution to δn_d is included in various integrals. To simplify further reduction, consider the usual case for which $z_d < \Delta$ and recall that $\epsilon = \epsilon_d - \omega_p^2/\tilde{\omega}^2$. Then after multiplying by ϵ_d and rearranging, (82) becomes

$$-\frac{\tilde{\omega}^2}{\omega_p^2}\epsilon_d\int_{-\infty}^{\infty} dz\, z\delta n_s(z) = -\int_{-\infty}^{z_d} dz\, z\delta n_s(z) - \epsilon_d\int_{z_d}^{\Delta} dz\, z\delta n_s(z) - \epsilon_d\Delta\int_{\Delta}^{\infty} dz\, \delta n_s(z) + (1-\epsilon_d)\left\{\left(-\frac{\tilde{\omega}^2}{\omega_p^2}\right)\epsilon z_d\frac{\sigma_s}{e} - z_d\int_{z_d}^{\infty} dz'\, \delta n_s(z') + \int_{-\infty}^{z_d} dz\, f(z)\left[-\frac{\tilde{\omega}^2}{\omega_p^2}\epsilon_d\frac{\sigma_s}{e} + \int_{-\infty}^{z} dz'\, \delta n_s(z')\right]\right\} \tag{83}$$

or

$$\left(1 - \frac{\tilde{\omega}^2}{\omega_p^2}\epsilon_d\right)\int_{-\infty}^{\infty} dz\, z\delta n_s(z) = \epsilon_d\int_{\Delta}^{\infty} dz\, (z-\Delta)\delta n_s(z) + (1-\epsilon_d)\left\{\int_{z_d}^{\infty} dz\, (z - z_d)\delta n_s(z) - \frac{\tilde{\omega}^2}{\omega_p^2}\frac{\sigma_s}{e}\left[\epsilon z_d + \epsilon_d\int_{-\infty}^{z_d} dz\, f(z)\right] + \int_{-\infty}^{z_d} dz\, f(z)\int_{-\infty}^{z} dz'\, \delta n_s(z')\right\} . \tag{84}$$

If instead $z_d > \Delta$, one finds

$$\left(1 - \frac{\tilde{\omega}^2}{\omega_p^2}\epsilon_d\right)\int_{-\infty}^{\infty} dz\, z\delta n_s(z) = \int_{\Delta}^{\infty} dz\, (z-\Delta)\delta n_s(z) + (1-\epsilon_d) \times\left\{\int_{-\infty}^{z_d} dz\, f(z)\int_{-\infty}^{z} dz'\, \delta n_s(z') - \frac{\tilde{\omega}^2}{\omega_p^2}\frac{\sigma_s}{e}\left[\epsilon\Delta + \epsilon_d\int_{-\infty}^{z_d} dz\, f(z)\right]\right\} . \tag{85}$$

Both (84) and (85) must be augmented on their right sides by

$$-\frac{\epsilon_d}{\omega_p^2}\int_{-\infty}^{\infty} dz\, \delta n_s(z)\, V'_{\rm xc}[n_0(z)] \ , \tag{86}$$

if one switches to a random phase approximation (RPA) response treatment.[23] In any case, the net result is that the dipole moment integral of δn_s has been written in terms of more numerically tractable integrals.

This feature continues to hold if we allow the d electrons to screen more than the Hartree term in the dynamic response. For such generalizations, we need to replace (66) with

$$-m\tilde{\omega}^2 \int_{-\infty}^{\infty} dZ\ Z\ \delta n_s(Z)$$
$$= \int_{-\infty}^{\infty} dZ\ \{\delta n_s(Z)\ [eE_+(Z) + eE_d(Z) + F_{\rm ext}(Z)]$$
$$+ n_0(Z)\ [eE_A + e\delta E_d(Z) + \delta F_{\rm ext}(Z)]\},$$

where E_d is the electric field produced by the ground state distribution of the d electrons and δE_d is the first order change in it, due to the system's response. We write

$$e(E_d + \delta E_d) = -\frac{\partial}{\partial Z}(V_d + \delta V_d)\ .$$

Similarly,

$$F_{\rm ext} + \delta F_{\rm ext} = -\frac{\partial}{\partial Z}(V_{\rm ext} + \delta V_{\rm ext})\ .$$

We consider only various approximations to local exchange-correlation energies as the possible sources of $V_{\rm ext} + \delta V_{\rm ext}$.

If there is partial d screening of the Hartree term in the ground state, we write

$$e\int dZ\ \delta n_s(Z) E_d(Z)$$
$$= -2\pi e^2 \int dZ \left(\frac{\partial}{\partial Z}\delta n_s(Z)\right) \int dZ'\ |Z - Z'| n_d(Z')\ . \tag{87}$$

The density n_d has both smooth and singular contributions [cf. Eq. (80) for its first order analog] and satisfies

$$\int dZ\ n_d(Z) = 0.$$

If there is partial d screening of the exchange-correlation potentials in the ground state, we write

$$\int dZ\ \delta n_s(Z)\ F_{\rm ext}(Z) = \int dZ \left(\frac{\partial}{\partial Z}\delta n_s(Z)\right) V_{\rm xc}^{\rm scr}(Z)\ . \tag{88}$$

An example of $V_{\rm xc}^{\rm scr}$ will be given below in Sec. IV. If there is partial d screening of the exchange-correlation potentials in the first order response, we write

$$\int dZ\ n_0(Z)\ \delta F_{\rm ext}(Z)$$
$$= \int dZ \left(\frac{\partial}{\partial Z} n_0(Z)\right) \delta n_s(Z)\ \frac{\partial}{\partial n}\ V_{\rm xc}^{\rm scr}(Z), \tag{89}$$

where n is evaluated as $n_0(Z)$ after the differentiation. We note that if there is no d screening of the exchange-correlation potentials in either the ground state or the response, then the contributions of the (88) and (89) terms above with ϵ_d everywhere unity should cancel.

IV. RESULTS AND DISCUSSION

A. Surface excitations in the q = 0 limit

We begin the presentation of our results by showing in Fig. 2 the frequency dependence of $d_\perp(\omega)$ and of the s and d contributions, $d_s(\omega)$ and $d_d(\omega)$. The boundary of the polarizable medium is assumed to coincide with the jellium edge, i.e., $z_d = 0$. The volume dielectric function of Ag is taken from the room temperature measurements of Hagemann *et al.*[26] and the s-electron density in bulk is described by $r_s = 2.97$. We determine $\epsilon_d(\omega)$ and $\epsilon_s(\omega) = 1 - \omega_p^2/[\omega(\omega + i\gamma)]$ from $\epsilon(\omega)$ as follows. Below the onset of interband transitions involving the $4d$ bands, $\epsilon_d(\omega)$ is real, so we fit $\gamma(\omega)$ by requiring $\mathrm{Im}\epsilon(\omega) = \mathrm{Im}\epsilon_s(\omega) \approx \gamma\omega_p^2/\omega^3$ and then find $\epsilon_d(\omega)$ by subtraction: $\epsilon_d(\omega) = \mathrm{Re}\,[\epsilon(\omega) - \epsilon_s(\omega)]$. Above the onset of interband transitions at $\omega = 3.7$ eV, we set $\gamma(\omega)$ from $\gamma\omega_p^2/\omega^3 = \mathrm{Im}\epsilon(\omega = 3.7\ \mathrm{eV})$ and find a complex valued $\epsilon_d(\omega)$ from $\epsilon_d(\omega) =$

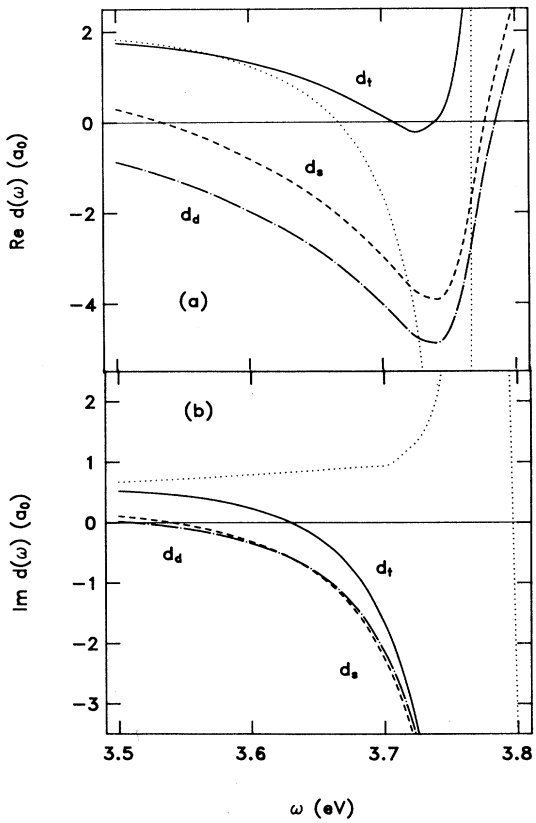

FIG. 2. Frequency dependence of (a) real and (b) imaginary parts of $d_\perp(\omega)$ calculated within TDLDA for two-component s-d electron system. Solid curves: total $d_\perp(\omega)$; dashed curves: $d_s(\omega)$; dash-dotted curves: $d_d(\omega)$. The boundary of the polarizable medium representing the d states is $z_d = 0$. The divergence of the d functions near ω_p^* is smoothed out, due to bulk damping processes. In the absence of the bulk broadening mechanisms, $\mathrm{Re}\,d(\omega) \to -\infty$ and $\mathrm{Im}\,d(\omega) \to +\infty$ for $\omega \to \omega_p^*$. The dotted curves indicate these divergences for $d_\perp(\omega)$.

$\epsilon(\omega) - \epsilon_s(\omega)$. Near ω_s^*, the bulk data give $\gamma \approx 0.3$ eV. This damping was included in the calculations shown in Fig. 2 by evaluating the dynamical surface response at complex frequencies, $\omega + i0.5\gamma$.

In principle, this relaxation-time treatment of damping processes is not quite correct, since it does not conserve the local electron density.[27] In a three-dimensional homogeneous electron gas, one finds corrections of the order of $0.5\gamma/\omega$. An extension to semi-infinite systems has not yet been attempted. If one assumes the surface corrections to be of the same magnitude as in the bulk, they would amount to less than 5%. We, therefore, ignore such modifications. Because of the damping, the divergence of $d_\perp(\omega)$ near the bulk plasma frequency is smoothed out. We have checked that, if γ is taken to be zero, $\mathrm{Re}\, d_\perp$ (as well as $\mathrm{Re}\, d_s$ and $\mathrm{Re}\, d_d$) approaches $-\infty$ for $\omega \to \omega_p^*$ (see dotted curve in Fig. 2). This behavior is also found on standard jellium surfaces and corresponds to the fact that, close to the transparency threshold, the induced charge is shifted deep into the interior.

The real part of $d_\perp(\omega)$ is seen to remain positive up to about 3.7 eV, i.e., until less than 2% below ω_p^*. This behavior is strikingly different from that at the standard jellium surfaces, where $\mathrm{Re}\, d_\perp(\omega)$ becomes negative already near the multipole surface plasma frequency, i.e., at about $0.8\omega_p$.[13,23,28] Thus, at the Ag surface plasma frequency (3.63 eV), we find $\mathrm{Re}\, d_\perp(\omega_s^*) \approx 1$ a.u., which is only slightly less than the static value 1.35 a.u. obtained for a standard jellium surface with $r_s = 2.97$. This demonstrates that screening at the surface of the two-component s-d electron system remains very efficient, until just below the transparency threshold. At low frequencies, the relative screening effect of the polarizable medium representing the $4d$ bands diminishes rapidly and the induced dipole moment approaches that of an ordinary jellium surface.

We point out that $\mathrm{Re}\, d_\perp$ remains positive up to much higher frequencies than the individual contributions, d_s and d_d, which turn negative near 3.54 and 3.26 eV, respectively. The reason is that the weight factors $c_s = (\epsilon_s - 1)/(\epsilon - 1)$ and $c_d = (\epsilon_d - 1)/(\epsilon - 1) = 1 - c_s$ in the expression $d_\perp = c_s d_s + c_d d_d$ [see (62)] have opposite signs. For example, at $\omega_s^* = 3.63$ eV, we have $c_s = (\epsilon_d + 1)/2 \approx 3$ and $c_d = 1 - c_s \approx -2$. This shows that there is no simple relationship between the effective induced dipole moment of the two-component s-d electron system and the centroid of the induced s-electron charge alone. In particular, the real parts of both d_s and d_d can be negative although the total $\mathrm{Re}\, d_\perp(\omega)$ is positive. This is indeed the case at $\omega = 3.63$ eV, where $\mathrm{Re}\, d_s = -1.4$ a.u. and $\mathrm{Re}\, d_d = -2.6$ a.u., whereas $\mathrm{Re}\, d_\perp = 1.0$ a.u.

Figure 2(b) shows the frequency dependence of the imaginary part of the total induced dipole moment and of its s and d contributions. In the absence of damping, $\mathrm{Im}\, d_\perp(\omega)$ (as well as the s and d contributions) remains positive up to the bulk plasma frequency (see dotted curve). As a result of the Drude damping, $\mathrm{Im}\, d_\perp$ is positive only up to about 3.63 eV; subsequently it becomes negative. As in the case of the real part, the imaginary part of the total induced dipole moment is not simply related to the imaginary parts of the s and d components. Thus, both of these contributions may be negative, while the total $\mathrm{Im}\, d_\perp$ is positive. The reason is again the rapid frequency variation and the opposite signs of the coefficients c_s and $c_d = 1 - c_s$.

We note here that, in the case of ordinary jellium surfaces, the cross section for photoabsorption, due to electronic surface excitations, is proportional to $\mathrm{Im}\, d_\perp(\omega)$.[13] Thus, this quantity must be positive below the bulk plasma frequency. If damping is included by evaluating the surface response at complex frequencies, $\mathrm{Im}\, d_\perp(\omega)$ does not need to remain positive, since this damping implies the presence of bulk absorption processes. These may interfere with surface excitations and lead to partial cancellations. Only the sum of both processes yields a positive definite total absorption rate.

The surface excitation spectrum shown in Fig. 2 does not show any evidence for the existence of a multipole surface plasmon. Because of the extreme closeness of the surface and volume plasma frequencies of the s-d electron system, an additional spectral feature between these main collective modes would in any case be difficult to discern. The extra broadening caused by the inclusion of bulk damping also implies that any such mode would probably be swamped by the tail of the monopole surface plasmon.

The induced s-electron density is shown in Fig. 3 for $\omega = 3.63$ eV, i.e., at the Ag surface plasma frequency. Plotted are the solutions using both approaches discussed in Sec. II. The agreement between these two methods is seen to be very good at this frequency. The slight differences probably stem from the use of different response kernels (short range in the first, long range in the second scheme). At slightly higher frequencies (as the bulk plasmon threshold is crossed), only the first scheme, evaluated with model densities,[23] gives reliable results, at least for the small damping factor γ that is used here. The induced density is dominated by a large peak within

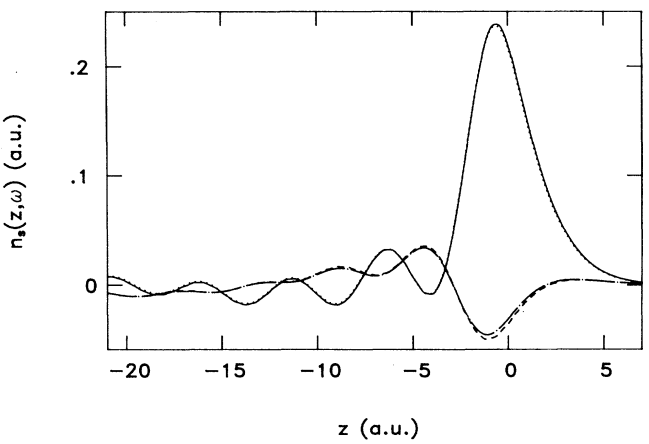

FIG. 3. Spatial distribution of normalized induced s-electron density $n_s(z,\omega)/\sigma(\omega)$ for $z_d = 0$, $r_s = 2.97$, and $\omega = 3.63$ eV. Solid (dashed) curve: real (imaginary) part using the first approach discussed in Sec. II; dotted (dash-dotted) curve: real (imaginary) part using second approach.

a few Å from the surface. Weaker short- and long-range Friedel oscillations decay rather slowly towards the interior. The centroid of the induced s-electron density is located slightly inside the metal for the case of Fig. 3. Nevertheless, as pointed out above, the total induced dipole moment is positive.

In order to compare more directly the s and d contributions to the dynamic surface response, we show in Fig. 4 the total induced polarization and the corresponding s and d polarizations for $\omega = 3.63$ eV. All curves are normalized to the total bulk polarization, which is given by $P_t(z \ll 0, \omega) = \sigma(\omega) = (\epsilon - 1)/(\epsilon + 1)$. Thus, plotted are

$$\bar{P}_s(z,\omega) = \int_z^\infty dz'\, \delta n_s(z',\omega)/\sigma(\omega) \tag{90}$$

and

$$\bar{P}_d(z,\omega) = \left(\sigma_d \frac{\epsilon}{\epsilon_d} - \frac{\epsilon_d - 1}{\epsilon_d} P_s(z,\omega)\right)\theta(z_d - z)/\sigma(\omega)\ , \tag{91}$$

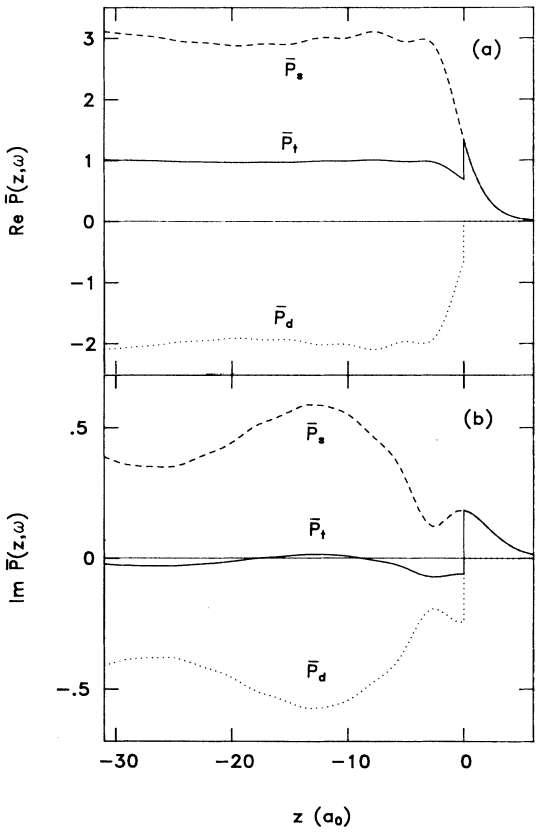

FIG. 4. Spatial distributions of (a) real and (b) imaginary parts of normalized induced polarizations for $z_d = 0$, $r_s = 2.97$, and $\omega = 3.63$ eV. Solid curves: total polarization $P_t(z,\omega)/\sigma(\omega)$; dashed curves: s-electron polarization $P_s(z,\omega)/\sigma(\omega)$; dotted curves: d-electron polarization $P_d(z,\omega)/\sigma(\omega)$. The asymptotic values of the s and d contributions are $c_s = 3.05 + i0.51$ and $c_d = 1 - c_s = -2.05 - i0.51$, respectively.

as well as $\bar{P}_t(z,\omega) = \bar{P}_s(z,\omega) + \bar{P}_d(z,\omega)$. Deep inside the metal, these functions approach the asymptotic values $\bar{P}_s(z \ll 0,\omega) = \sigma_s/\sigma = c_s = 3.05 + i0.51$ and $\bar{P}_d(z \ll 0,\omega) = \sigma_d/\sigma = c_d = -2.05 - i0.51$, i.e., the normalized total polarization in the interior is $c_s + c_d = 1$.

The polarization of the d states has the opposite sign of the s-electron polarization and, therefore, causes a drastic cancellation. The main screening effect takes place within a few Å from the surface; deeper inside, all polarizations exhibit characteristic Friedel oscillations about their mean asymptotic values. The discontinuities in $P_d(z,\omega)$ and $P_t(z,\omega)$ at $z = z_d = 0$ are caused by the sheet of d-electron screening charge located at the edge of the polarizable medium.

As mentioned in the Introduction, a two-component s-d electron system (without damping in ϵ_s) has been used previously by one of the authors[11] to evaluate surface excitation spectra at finite q parallel to the surface plane and to determine the dispersion of the surface plasmon. At finite q, the surface excitations can be derived from the imaginary part of the surface response function $g(q,\omega)$, which is defined as the asymptotic amplitude of the induced electric potential far from the surface:

$$\phi(z,q,\omega) \to -\frac{2\pi}{q}\left[e^{qz} - g(q,\omega)\, e^{-qz}\right]\ . \tag{92}$$

In the limit of small q, this response function should be related to the d parameters in the following manner:[13,14]

$$g(q,\omega) = \frac{\epsilon(\omega) - 1}{\epsilon(\omega) + 1 - 2q[\epsilon(\omega) d_\perp(\omega) + d_\parallel(\omega)]}\ . \tag{93}$$

We have found that the two calculational approaches, one based on the direct evaluation of $g(q,\omega)$ in the region $q \geq 0.05$ Å^{-1} and the other using the above formula together with the d parameters, are in fact compatible. This is illustrated in Fig. 5, where the frequency dependence of $\mathrm{Im}\, g(q,\omega)$ is shown for $q = 0.05$ Å^{-1}. The dashed curve is obtained from the full surface response function, while the dotted curve corresponds to the small-q expansion (93) using $d_\perp$. We have again set $z_d = 0$, so that $d_\parallel = 0$ according to (53). Also plotted is the $q = 0$ spectrum, i.e., $\mathrm{Im}\{[\epsilon(\omega) - 1]/[\epsilon(\omega) + 1]\}$ (solid curve). The agreement between the two calculations at finite q is seen to be very good, indicating that both approaches are perfectly consistent as long as $d_\perp(\omega)$ and $g(q,\omega)$ are evaluated within the same model.

The spectra shown in Fig. 5 reveal no trace of the multipole surface plasmon. As mentioned above, this mode is presumably suppressed, because of the closeness of the surface and volume plasma frequencies in Ag, and because of the extra broadening caused by the bulk damping processes.

B. Surface plasmon dispersion: Comparison with experiment

We now turn to the comparison of the calculated surface plasmon dispersion with the experimental results. Figure 6 shows $\omega_s^*(q)$ as derived within the same model

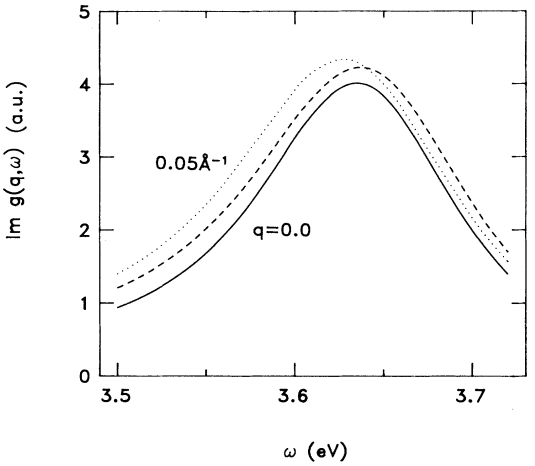

FIG. 5. Spectral distribution of surface excitations of a two-component s-d electron system. Solid curve: $q = 0$ limit, i.e., $\mathrm{Im}\,(\epsilon-1)/(\epsilon+1)$, where $\epsilon(\omega)$ is the measured bulk dielectric function (Ref. 26); dashed curve: $\mathrm{Im}\,g(q,\omega)$ at $q = 0.05$ Å^{-1}, as calculated within TDLDA (Ref. 11); dotted curve: $\mathrm{Im}\,g(q,\omega)$ at $q = 0.05$ Å^{-1} derived from small-q expansion (93), with $d_\perp(\omega)$ as in Fig. 2.

as discussed above together with the analogous results when the polarizable medium representing the d states is terminated at $z_d = -0.8$ Å. The $\omega_s^*(q)$ are determined from the frequency location of peaks in $\mathrm{Im}\,g(q,\omega)$ at fixed q. The short curves close to the origin are obtained from the d parameters and the approximation (93), while the

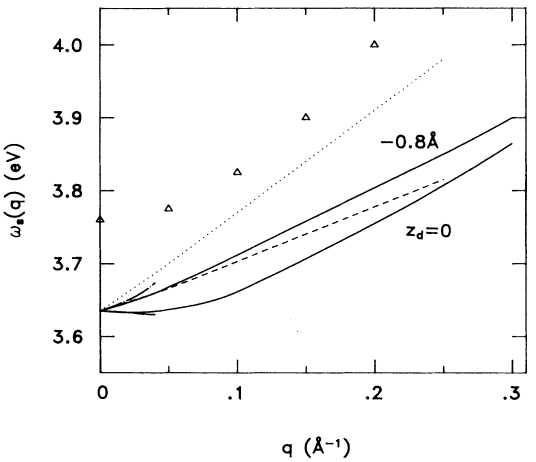

FIG. 6. Dispersion of Ag surface plasmon. The theoretical results are for the Lang-Kohn ground state (no s-d screening included), with the finite-frequency response treated within the TDLDA with only the Hartree term screened via the s-d polarization. Solid curves: finite-q calculations for $z_d = 0$ and $z_d = -0.8$ Å. The short curves close to the origin denote the corresponding results obtained from the d parameters. The dotted and dashed curves denote the measured dispersions for Ag(100) and Ag(111), respectively. The experimental results for the anisotropic (110) face lie close to the (100) and (111) data. The triangles indicate the measured dispersion of the Ag bulk plasmon.

remaining curves result from using the full finite-q surface response function $g(q,\omega)$ over the q range from 0.05 to 0.3 Å^{-}1. All results are based on the Lang-Kohn equilibrium density profile and the TDLDA response with only the Hartree contribution to the induced potential screened by the d states. Also indicated are the measured dispersions for Ag(100) and Ag(111). The two experimental curves for the anisotropic (110) face lie close to the (100) and (111) data. These data have been shifted down by 0.06 eV in order to match the value of $\omega_s^*(q = 0)$ obtained from the measured bulk dielectric function.[26] For the sake of completeness, we also plot the dispersion of the bulk plasmon,[29] which is seen to lie slightly above the surface plasmons.

For $z_d = -0.8$ Å, the calculated dispersion is seen to lie within the range of the measured results. In particular, the weak minimum at small q has disappeared. Both $d_\perp$ and $d_\parallel$ contribute significantly to the upward dispersion; e.g., at 3.63 eV, we find $d_\perp = -0.77 - 1.16i$ and $d_\parallel = 3.17 + 0.79i$. The physical origin of the blueshift relative to the theoretical results for $z_d = 0$ is that a larger portion of the charge density associated with the surface plasmon fluctuates outside the range of the polarizable d medium. Although the equilibrium density is reduced in this selvedge region [which for simple metals leads to a negative dispersion up to about $q = 0.15$ Å^{-1} (Ref. 8)], the reduction of the s-d interaction in the same region is the stronger effect and leads to a q dependent upward shift towards the unscreened plasma frequencies. In the nonretarded limit, the $q = 0$ value $\omega_s^* = 3.63$ eV is, of course, independent of z_d. We note here that, if z_d is shifted deeper inside the metal, the initial slope of the Ag surface plasmon becomes more and more positive, since the unscreened plasma frequency near 6.5 eV must be approached.

It is remarkable, that for $z_d = -0.8$ Å, the initial slope derived from the d functions is similar to the overall slope at larger q obtained from the full $g(q,\omega)$. This does not imply, however, that the large-q region is governed by the same processes as the small-q region. The comparison with the results for $z_d = 0$ illustrates quite convincingly that these two regions (roughly separated at $q = 0.05$ Å^{-1}) have generally distinct behavior. Also, as we discuss below, these two regions depend differently on the ground state electronic properties and on modifications of the dynamical response calculation.

Because of the simplicity of the present s-d electron system, it is not clear whether a direct physical meaning can be attached to the location of the parameter z_d. Since z_d is determined not only by the equilibrium location of the d electrons, but also by the spatial extent of their response, it is not a ground state quantity and can, therefore, not be simply equated, for example, with the distance of the first atomic plane from the jellium edge. Microscopically, a single plane of Ag atoms should have a less sharp onset of interband transitions than a three-dimensional crystal. The surface of a semi-infinite Ag crystal might be viewed as an intermediate case, in particular, at finite q, where the penetration depth of the plasmon field is exponentially reduced. A less sharp on-

set of interband transitions should lead to a reduction of the real part of ϵ_d below the onset and a corresponding blueshift of the surface plasma frequency: According to the formula $\omega_s^* = \omega_p/\sqrt{1+\epsilon_d}$, a decrease of ϵ_d from 5 to 4 causes ω_s^* to increase by 0.35 eV, i.e., by more than the entire q dispersion observed on the three low-index faces of Ag. An inward shift of z_d can be interpreted as a reduction of ϵ_d from its bulk value (≈ 5) to unity in the thin surface region $z_d < z \leq 0$. Thus, a tentative rationalization of the position $z_d = -0.8$ Å used in Fig. 6 could be that the interband onset is weakened at the surface due to finite-size effects.

The above picture can in fact be used to argue that the surface plasma frequency on the (100) face should lie above that for the (111) face, just as it is experimentally observed. Since the atomic density within a (100) plane is smaller than in the densely packed (111) plane, ϵ_d should be reduced more, or should be reduced over a wider region, in order to simulate the reduced strength of the interband transition relative to the bulk situation. Shifting z_d farther inside leads to an enhanced blueshift in agreement with the measurements. Conversely, one might argue that on the (111) face, ϵ_d should be reduced less, or only over a thinner region, since the strength of the interband transition should be more similar to the bulk case. Thus, the plasma frequency should be less blueshifted than on Ag(100). But according to this simple argument, the frequency on Ag(110) should be even higher than on Ag(100), since the intraplanar atomic density is even lower. The data, however, show that this is not the case. The nonmonotonic behavior of the dispersions seen on the three low-index faces clearly suggests that no one-parameter model can provide a satisfactory explanation. Moreover, the anisotropy observed on Ag(110) is a measure of the importance of $d_{\parallel}$. It is plausible that this parameter should also differ for the three low-index faces. Thus, a consistent understanding of the face dependence of the dispersions cannot be achieved solely in terms of $d_{\perp}$.

It would be very interesting to investigate whether optical data, for which the corrections to classical optics are determined by the d parameters, can also be better reproduced with an effective d-electron medium terminated below rather than at the jellium edge. For example, the positive slope that we find here for $z_d = -0.8$ Å implies that the Ag surface plasmon polariton frequencies in the retardation regime should lie above the values expected within the local Fresnel picture. In the latter case, the plasmon polariton dispersion is determined by the relation

$$\kappa' + \kappa\epsilon = 0 \ , \tag{94}$$

where

$$\kappa = \sqrt{q_x^2 - \frac{\omega^2}{c^2}} \ ,$$

$$\kappa' = \sqrt{q_x^2 - \epsilon\frac{\omega^2}{c^2}} \ .$$

For a given ω, the parallel wave vector is then determined by

$$q_x^2 = \frac{\omega^2}{c^2}\frac{\epsilon(\omega)}{\epsilon(\omega)+1} \ . \tag{95}$$

In the presence of nonlocal surface corrections, the relation (94) is replaced by the condition[30]

$$\kappa' + \kappa\epsilon = (\epsilon - 1)\left[q_x^2 d_{\perp} - \kappa\kappa' d_{\parallel}\right] \ . \tag{96}$$

For not too small values of $1/|\epsilon|$ and $|\epsilon+1|$, these corrections imply

$$q_x' = q_x\left(1 - \frac{\sqrt{-\epsilon}}{\epsilon+1}\, q_x \,\mathrm{Re}[d_{\perp} - d_{\parallel}] + O(q_x^2)\right) \ , \tag{97}$$

where q_x is defined in (95). Thus, at a given frequency below ω_s^*, q_x should be reduced if $\mathrm{Re}\,[d_{\perp} - d_{\parallel}] < 0$. The attenuated reflection data on Ag by Tadjeddine *et al.*[31] show the opposite trend, since the observed polariton frequencies are smaller than expected from classical theory if the optical data of Hagemann *et al.*[26] or Johnson and Christy[32] are used. This effect could be related to the fact that these measurements were not done under UHV conditions. Small amounts of a surface oxide might lead to a lowering of the polariton frequencies. We point out, however, that this analysis depends sensitively on the accuracy of the bulk dielectric function. Thus, the bulk ϵ quoted in Ref. 31 gives a Fresnel dispersion below rather than above the measured polariton curves.

C. Sensitivity to model assumptions

Since the two-component s-d electron system represents a highly simplified model of the actual dynamical response occuring at Ag single crystal surfaces, it is important to inquire to what extent the model predictions depend on the input assumptions. As discussed above, variations of the boundary z_d do not alter the qualitative picture, but do lead to significant changes in detail. Also, in Ref. 11 it was shown that an RPA response formulation yields slightly higher surface plasma frequencies for $q > 0$ than the TDLDA because, in the latter case, the bare Coulomb interaction (screened via the s-d polarization) is partially diminished by the exchange-correlation contributions to the complex local potential. The shifts are, however, rather small so that the overall picture remains the same.

Since the ground state electronic density in the calculations discussed above corresponds to the standard jellium model by Lang and Kohn,[20] the treatment of electron interactions, in the presence and absence of the applied electromagnetic field, is, in fact, not quite consistent. Figure 7 shows how the ground state density profile and the effective one-electron potential are modified if the s-d polarization is included in the interior of the metal. Screening of only the Hartree potential and of both Hartree and exchange-correlation potentials are considered. For both cases, the Poisson equation away from $z = z_d$ is

$$\phi_0''(z) = -4\pi\left[n_0(z) - n_+(z)\right]/\epsilon_d(z) \ , \tag{98}$$

where $\epsilon_d(z) = \epsilon_d = 4$ for $z \leq z_d$ and $\epsilon_d(z) = 1$ for $z > z_d$.

The value $\epsilon_d = 4$ corresponds roughly to the adiabatic limit of the d electron contribution derived from optical data.[26] In the second case, not only the Hartree, but also the local exchange-correlation potential is screened. We account for this additional screening by writing $V_{xc}^{scr} = V_x^{scr} + V_c^{scr}$, where

$$V_x^{scr}(z) = V_x^{bare}(z)/\epsilon_d(z) \ , \tag{99}$$

and

$$V_c^{scr}(z) = V_x^{scr}(z)\ f[r_s(z)/\epsilon_d(z)] \ . \tag{100}$$

If the Wigner interpolation formula is used, one has

$$f(x) = 0.72x\ \frac{4x/3 + 7.8}{(x+7.8)^2} \ . \tag{101}$$

The discontinuity in $\epsilon_d(z)$ leads to a discontinuity of V_{xc}^{scr} and a strong distortion of the s-electron equilibrium density profile, although the total barrier height is just slightly changed. When the d electrons screen only the Hartree potential, the changes in n_0 and V are less noticeable.

We point out that the overall height of the surface barrier changes a little as a result of these different ground state treatments. Thus, the work function Φ, which is of crucial importance for the screening properties of metallic surfaces, is nearly the same for the cases shown in Fig. 7. Once the boundary of the d medium is moved outside the jellium edge, however, Φ diminishes quite rapidly, because of the strong reduction of the surface dipole.

The variation of the work function Φ as a result of the s-d polarization in the ground state when $z_d = 0$ is shown in Fig. 8. If only the Hartree potential is screened, Φ decreases monotonically from 3.5 eV to about 3.4 eV as ϵ_d is increased from 1 to 5. This decrease reflects the reduction of the surface dipole, due to the s-d polarization in the region $z \leq z_d$. On the other hand, if V_{xc} is also screened, the work function exhibits a sharp minimum near $\epsilon_d = 1.5$ and a subsequent increase. This more complex behavior is related to the fact that Φ depends not only on the surface dipole (which is influenced by both Coulomb and exchange-correlation terms), but also on the bulk exchange-correlation potential. As shown by Lang and Kohn,[20] Φ may be expressed as

$$\Phi = D + V_{xc}^{scr}(\infty) - V_{xc}^{scr}(-\infty) - E_F \ . \tag{102}$$

In the present case where $z_d = 0$, the surface dipole is given by

$$D = 4\pi \int_{-\infty}^{\infty} z\ [n_0(z) - n_+(z)]/\epsilon_d(z) \ . \tag{103}$$

Since D and V_{xc}^{scr} depend differently on ϵ_d, a nonmonotonic variation of $\Phi(\epsilon_d)$ is not surprising. There are similar variations in Φ with z_d at a fixed value of ϵ_d.

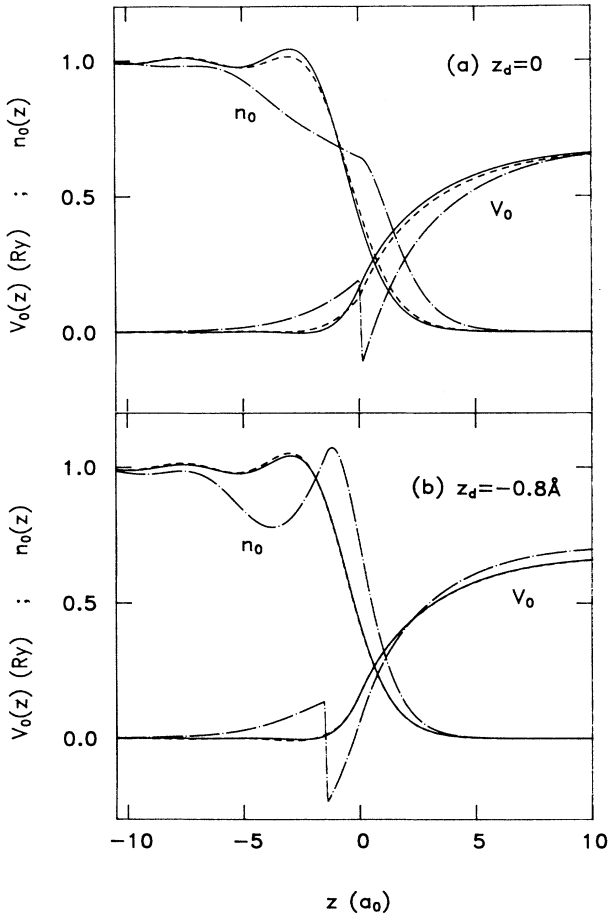

FIG. 7. Normalized ground state density profiles and one-electron potentials for different treatments of electron interactions. Solid curve: standard Lang-Kohn jellium model; dashed curve: Hartree potential screened via s-d polarization; dot-dashed curve: both Hartree and exchange-correlation potentials screened via s-d polarization. In both cases $\epsilon_d = 4$, while in (a) $z_d = 0$ and in (b) $z_d = -0.8$ Å.

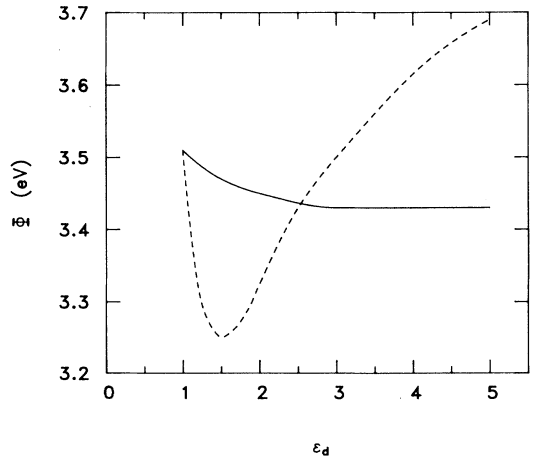

FIG. 8. Work function Φ for $r_s = 2.97$ jellium surface as a function of dielectric constant of polarizable medium extending up to $z_d = 0$. Solid curve: Hartree potential screened via s-d polarization; dashed curve: both Hartree and exchange-correlation potentials screened via s-d polarization.

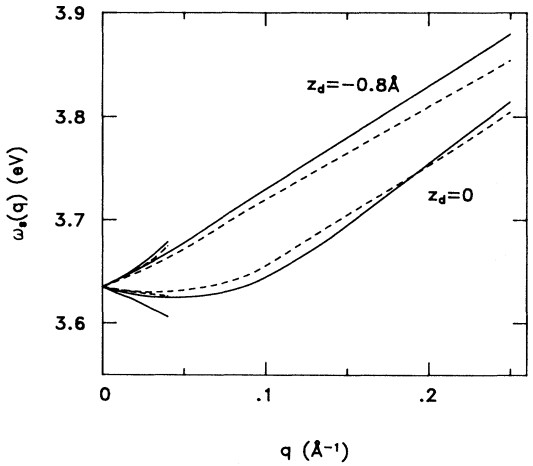

FIG. 9. Dispersion of Ag surface plasmon for two consistent treatments of electron interactions in the ground state and for the finite-frequency response: *s-d* screening included only in Hartree potential (solid curve) and in both Hartree and exchange-correlation potentials (dashed curve). The short curves close to the origin denote the results obtained from the *d* parameters, the remaining curves are derived from the full surface response function $g(q,\omega)$. All results are calculated within the TDLDA, modified by the *s-d* screening. The lower pair of results have $z_d = 0$, while the upper pair use $z_d = -0.8$ Å.

Figure 9 shows the dispersion of the Ag surface plasmon for two consistent treatments of electron-electron interactions in the ground state and in the presence of the applied field: *s-d* polarization included only in the Hartree term (solid curve) and in both Hartree and exchange-correlation terms (dashed curve). The calculations have been done for z_d values of both 0 and −0.8 Å. The short curves close to the origin denote again the results obtained from the *d* parameters, while the remaining curves give the dispersions derived from the general $g(q,\omega)$ within the q range from 0.05 to 0.25 Å^{-1}. Comparing the results for $z_d = 0$ with those in Fig. 6, it is evident that the qualitative picture is not altered, due to these different treatments of electron interactions. The similarity of the *d's* is surprising, since the ground state profiles shown in Fig. 7 are clearly different. Indeed the profiles of the induced charge densities are quite different, but their centroids are not.

The analogous dispersions for $z_d = -0.8$ Å are also plotted in Fig. 9. As in Fig. 6, the weak minimum at small q has disappeared and the dispersion is positive over the entire q range in approximate agreement with the measured dispersions. As before, the inward shift of z_d causes an enhancement of the blueshift. Thus, within the present model, the overall behavior of the q dependence of the Ag surface plasmon seems to be overwhelmingly dominated by the fundamental q dependence of the mutual *s-d* polarization in the surface region.

V. SUMMARY

The *d* parameters that characterize the nonlocal optical response of metal surfaces have been evaluated for a two-component *s-d* electron system. The *s* electrons are treated as a semi-infinite electron gas, while the occupied *d* states are represented in terms of a polarizable half space. To be able to numerically calculate the induced dipole moments in the $q_{\|} = 0$ limit in a stable manner, the dynamical force sum rule, which was previously known only for pure *s* electron systems, has been generalized. The resulting *d* functions are shown to give an initial slope of the surface plasmon that is consistent with the finite-q dispersion obtained from the full surface response function g.

If the boundary z_d of the polarizable half space coincides with the jellium edge, the initial slope is found to be slightly negative although the overall dispersion for $q > 0.05$ Å^{-1} is positive. Thus, the linear region is rather small and cannot be taken as representative of the main parallel momentum region in which the experimental data are observed ($q \leq 0.3$ Å^{-1}). If the boundary is moved inside the metal, the initial slope also becomes positive and the overall dispersion agrees qualitatively with the dispersions observed on the three low-index faces of Ag.

Various alternative treatments of the *s-d* polarization in the ground state and in the finite-frequency response are shown to lead to minor modifications of the calculated dispersion. These results, therefore, support the main physical picture for the Ag surface plasmon dispersion that was proposed earlier by one of the authors:[11] The mutual *s-d* polarization that is responsible for the large downward shift of the Ag surface collective modes is gradually switched off at finite parallel momenta, because of the reduced penetration depth of the plasmon field.

It would be very interesting to check whether optical data are consistent with the positive slope of the surface plasmon in the small-q region. Also, refinements of the present two-component *s-d* electron model that allow the consideration of the face dependence of the dispersion [including its anisotropy on the (110) face] would be desirable.

[1] A. Liebsch, in *Photonic Probes of Surfaces*, edited by P. Halevi (Elsevier, Amsterdam, 1995).

[2] K.D. Tsuei, E.W. Plummer, A. Liebsch, K. Kempa, and P. Bakshi, Phys. Rev. Lett. **64**, 44 (1990); K.D. Tsuei, E.W. Plummer, A. Liebsch, E. Pehlke, K. Kempa, and P. Bakshi, Surf. Sci. **247**, 302 (1991).

[3] H.J. Levinson, E.W. Plummer, and P.J. Feibelman, Phys. Rev. Lett. **43**, 952 (1979); H. J. Levinson and E.W. Plummer, Phys. Rev. B **24**, 628 (1981).

[4] A. Liebsch and W.L. Schaich, Phys. Rev. B **40**, 5401 (1989).

[5] A. Zangwill and P. Soven, Phys. Rev. A **21**, 1561 (1980);

M.J. Stott and E. Zaremba, *ibid.* **21**, 121 (1980); G. Mahan, *ibid.* **22**, 1780 (1980).

[6] J.T. Lee and W.L. Schaich, Phys. Rev. B **43**, 4629 (1991); K. Burke and W.L. Schaich, *ibid.* **48**, 14 599 (1993); H. Ishida and A. Liebsch, *ibid.* **50**, 4834 (1994); K. Burke and W.L. Schaich, *ibid.* **49**, 11 397 (1994); D. Samuelson and W. Schattke, *ibid.* **51**, 2537 (1995); Surf. Sci. **327**, 379 (1995).

[7] R. Contini and J.M. Layet, Solid State Commun. **64**, 1179 (1987); S. Suto, K.D. Tsuei, E.W. Plummer, and E. Burstein, Phys. Rev. Lett. **63**, 2590 (1989); G. Lee, P.T. Sprunger, E.W. Plummer, and S. Suto, *ibid.* **67**, C3198 (1991); H. Rocca *et al.*, *ibid.* **64**, 2398 (1990); **67**, C3197 (1991); **69**, 2122 (1992).

[8] P.J. Feibelman, Phys. Rev. B **40**, 2752 (1989); K.D. Tsuei, E.W. Plummer, and P.J. Feibelman, Phys. Rev. Lett. **63**, 2256 (1989).

[9] H. Ehrenreich and H.R. Philipp, Phys. Rev. **128**, 1622 (1962). See also, D. Pines, *Elementary Excitations in Solids* (Benjamin, New York, 1964).

[10] U. Kreibig and L. Genzel, Surf. Sci. **156**, 678 (1985).

[11] A. Liebsch, Phys. Rev. Lett. **71**, 145 (1993); Phys. Rev. B **48**, 11 317 (1993).

[12] J. Tiggesbäumker, L. Köller, K.H. Meiwes-Broer, and A. Liebsch, Phys. Rev. A **48**, 1749 (1993); see also, V. Kresin, Phys. Rev. B **51**, 1844 (1995).

[13] P.J. Feibelman, Prog. Surf. Sci. **12**, 287 (1982).

[14] W.L. Schaich and W. Chen, Phys. Rev. B **39**, 10 714 (1989).

[15] E. Zaremba and W. Kohn, Phys. Rev. B **13**, 2270 (1976).

[16] P. Apell and C. Holmberg, Solid State Commun. **49**, 693 (1984).

[17] J. Tarriba and W.L. Mochan, Phys. Rev. B **46**, 12 902 (1992).

[18] Y. Borensztein, W.L. Mochan, J. Tarriba, R.G. Barrera, and A. Tadjeddine, Phys. Rev. Lett. **71**, 2334 (1993).

[19] P.J. Feibelman, Surf. Sci. **282**, 129 (1993); Phys. Rev. Lett. **72**, C788 (1994).

[20] N.D. Lang and W. Kohn, Phys. Rev. B **1**, 4555 (1970).

[21] A. Liebsch, Phys. Rev. Lett. **72**, C789 (1994).

[22] R.S. Sorbello, Solid State Commun. **56**, 821 (1985); S.T. Epstein and R.E. Johnson, J. Chem. Phys. **51**, 188 (1969).

[23] A. Liebsch, Phys. Rev. B **36**, 7378 (1987).

[24] W.L. Schaich, Phys. Rev. B **47**, 14 599 (1993).

[25] W.L. Schaich, Phys. Rev. B **50**, 17 587 (1994).

[26] H.J. Hagemann, W. Gudat, and C. Kunz, J. Opt. Soc. Am. **65**, 742 (1975).

[27] N.D. Mermin, Phys. Rev. B **1**, 2362 (1970).

[28] K. Kempa and W.L. Schaich, Phys. Rev. B **37**, 6711 (1988).

[29] P. Zacharias and K.L. Kliewer, Solid State Commun. **18**, 23 (1976).

[30] P. Apell, Phys. Scr. **24**, 795 (1981).

[31] A. Tadjeddine, D.M. Kolb, and R. Kötz, Surf. Sci. **101**, 277 (1980).

[32] P.B. Johnson and R.W. Christy, Phys. Rev. B **6**, 4370 (1972).